RSC Advances

REVIEW

View Article Online
View Journal | View Issue

Cite this: *RSC Adv.*, 2014, **4**, 29012

Organo-metal perovskite based solar cells: sensitized *versus* planar architecture

Shany Gamliel and Lioz Etgar*

Organo-metal halide perovskites are composed of an ABX3 structure in which A represents a cation, B a divalent metal cation and X a halide. The organo-metal perovskite shows very good potential to be used as a light harvester in solar cells due to its direct band gap, large absorption coefficient, high carrier mobility and good stability. However, there is an important question in the photovoltaic field regarding the most advantageous architecture for perovskite based solar cells. Several studies showed sensitized perovskite solar cells achieving high performance, while high efficiency was also observed with the planar architecture. Consequently, it is still an open question regarding which operation mechanism and which architecture offers better results. This review describes both architectures, based on studies in the field. In the case of the sensitized structure, there are more difficulties in pore filling, naturally more recombination, and the possibility to use thicker metal oxide films. In the planar structure, thin metal oxide films are used, less recombination was observed and there are no infiltration problems. Both architectures exhibit long-range diffusion length and meet the demand for excellent coverage of the perovskite film.

Received 30th April 2014
Accepted 19th June 2014

DOI: 10.1039/c4ra03981e

www.rsc.org/advances

1. Introduction

In recent years a breakthrough has occurred in the photovoltaic field—the use of organic–inorganic perovskites as a light harvester in solar cells. The organo-metal halide perovskite solar cell has the potential of replacing current technologies due to its simple preparation, low cost, superior optical properties and high stability. Currently, much research is devoted to this issue, and researchers from various fields are involved, including theoreticians, chemists, physicists and engineers.

The most common perovskite used for PV application is the methyl ammonium lead halide ($CH_3NH_3PbX_3$, X = Br, Cl, I), already proposed in 2009 as an efficient light harvester in liquid solar cells.[1] Since then, photovoltaic performance has increased dramatically achieving efficiency of more than 16%.[2–5]

The Hebrew University of Jerusalem, Institute of Chemistry, Casali Center for Applied Chemistry, Israel. E-mail: lioz.etgar@mail.huji.ac.il

Shany Gamliel is an M.Sc. student at Dr Lioz Etgar's lab at the Institute of Chemistry in the Hebrew University of Jerusalem, Israel. She received her B.Sc degree in chemistry from Brooklyn College, NYC, while researching polymorphic liquids and glasses through computer simulation. Her current research interests are hole conductor free perovskite solar cells, perovskite materials and nanomaterials.

Lioz Etgar obtained his Ph.D. (2009) at the Technion-Israel Institute of Technology and was post-doc with Prof. Michael Grätzel (2009–2012) at EPFL, Switzerland. During his post-doc he received a Marie Curie Fellowship, and won the Wolf Prize for young scientists. Since 2012 he has been a senior lecturer in the Institute of Chemistry at the Hebrew University. Etgar's research group is focusing on the development of innovative solar cells. He is seeking new excitonic solar cell structures/architectures with design and control of the inorganic sensitizer structure and properties in order to improve the PV parameters.

The possibility to tune the optical properties of the organo-metal halide perovskite paves the way to high voltage cells. Open circuit voltage (V_{oc}) of 1.15 V and 1.3 V using $CH_3NH_3PBr_3$ as a light harvester with various hole transport materials has been demonstrated.[6,7]

It may seem obvious to consider perovskite-based solar cells as a new kind of dye sensitized solar cells (DSSC). However, several reports shed new light on high efficiency planar perovskite-based solar cells. Are perovskite-based solar cells more like sensitized solar cells, or planar heterojunction solar cells? In this review, we present research from both points of view, describing the advantages and disadvantages of sensitized perovskite solar cells and planar perovskite solar cells.

2. Crystal structure of organo-metal halide perovskite

One of the pioneer studies on the perovskite structure was conducted in the 1920s.[8] The crystal structure of the ideal perovskite (the 3D perovskite crystal structure) is cubic ABX3 consisting of corner sharing (BX6) octahedra with the A cation occupying 12-fold coordination site. The B cation is a divalent metal, which satisfies the charge balancing. Examples for the metal cation include: Cu_2^{2+}, Ni_2^{2+}, Co_2^{2+}, Fe_2^{2+}, Mn_2^{2+}, Cr_2^{2+}, Pd_2^{2+}, Cd_2^{2+}, Ge_2^{2+}, Sn_2^{2+}, Pb_2^{2+}, Eu_2^{2+}, or Yb_2^{2+}. The basic structures of organo-metal perovskite are $(R\text{–}NH_3)_2MX_4$ and (NH–R–NH)MX; ($X = Cl^{-1}$, Br^{-1}, or I^{-1}).[9]

Moreover, the organic component can consist of a bilayer or a monolayer of organic cations. The ammonium head (in the case of monoammonium) of the cation component bonds to the halogens in one inorganic layer, and the organic group extends into the space between the inorganic layers.

The organic groups are optically inert and function as "spacer" groups by that allowing the ABX_3 lattice to be maintained; however, they have a major influence on the properties of the perovskite. The organic component tunes the binding exciton energy as it influences the dielectric constant. Currently several reports showed the replacement of the commonly used methyammonium cation by the formamidinium cation, achieving broadly tunable absorption spectra.[10] Additionally, by changing the halides, the optical properties of the perovskite can be tuned, achieving absorption at different wavelengths.[11,41]

Organo-metal halide perovskite has good potential to be used as a light harvester in the solar cell due to its direct band gap, large absorption coefficients[12] and high carrier mobility.[13,14]

3. Sensitized perovskite based solar cells

Fig. 1 describes the solar cell structure of a perovskite sensitized solar cell when the perovskite penetrates through the mesoporous metal oxide (commonly TiO_2). In this cell structure, there is close contact between the perovskite and the metal oxide, through almost all the film thickness. This section describes several studies on perovskite solar cells based on mesoporous metal oxide.

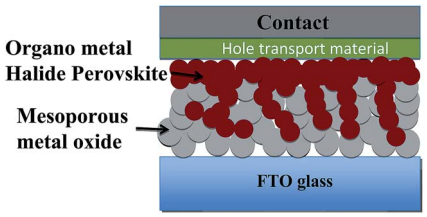

Fig. 1 Structure of sensitized perovskite solar cell.

3.1 Liquid electrolyte

Early work by Miyasaka *et al.*[1] reported on organo-metal nanocrystals sensitized-TiO_2 for solar cells. The authors used the $CH_3NH_3PbBr_3$ and $CH_3NH_3PbI_3$ as sensitizers on mesoporous TiO_2 with liquid electrolyte achieving power conversion efficiency (PCE) of 3.18% with spectral response covering the whole visible region till 800 nm. In a later work, Park *et al.*[15] used 2–3 nm perovskite nanoparticles sensitized on 3.6 μm-thick TiO_2 with iodide/iodine based redox electrolyte. The solar cell efficiency was improved, achieving 6.5% with maximum external quantum efficiency (EQE) of 78.6% at 530 nm.

Zhao *et al.*[16] studied the effect of TiO_2 film thickness (1.8–8.3 μm) on the charge transport, recombination, and device characteristics of perovskite ($CH_3NH_3PbI_3$), sensitized solar cells using iodide-based electrolytes. They showed that using electrolytes with low concentration results in relatively stable solar cells. On the other hand, polar electrolytes or higher iodide concentrations of nonpolar electrolytes achieved higher cell performances, but result in degradation or bleaching of the $CH_3NH_3PbI_3$. In addition, when increasing the TiO_2 film thickness, although the absorption increases the overall cell performance current density (J_{SC}), fill factor (FF), open circuit voltage (V_{oc}), and efficiency (η) were decreased.

Incident modulated voltage spectroscopy (IMVS) and intensity modulated photocurrent spectroscopy (IMPS) measurements were performed to investigate the charge transport and recombination process (Fig. 2). No significant effect of TiO_2 film thickness on electron diffusion coefficient was observed. Yet the electron recombination lifetime (τ) is strongly dependent on the TiO_2 film thickness. The decrease in electron recombination was attributed to the low electrolyte concentration (0.08 M) of I^- compared to the standard concentration (0.5–1 M) of electrolytes. Thus, the depletion of I^- enhanced within the TiO_2 pores with increasing TiO_2 film thickness; the diffusion pathway through the pores elongated with increasing TiO_2 film thickness. Moreover, the increases in electron recombination with increasing TiO_2 film thickness can be explained by increased I^- deficiency with increasing TiO_2 film thickness.

3.2 Hole transport material

Changing the liquid electrolyte to solid state hole transport material (HTM) improved the stability of the cells and enhanced

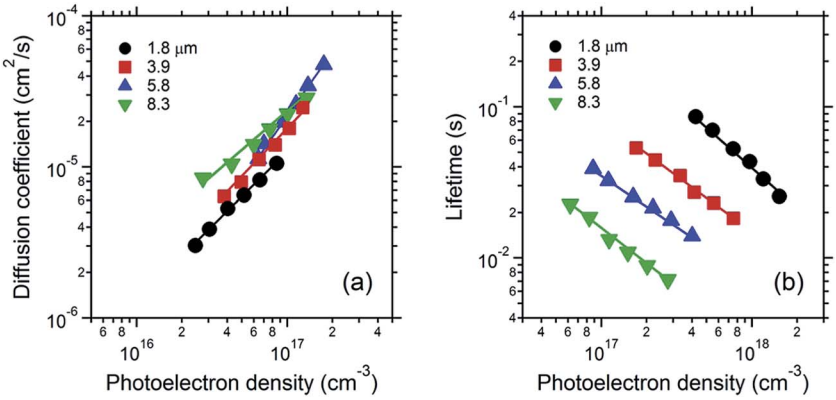

Fig. 2 Effect of TiO_2 film thickness on the (a) electron diffusion coefficient and (b) recombination lifetime for $(CH_3NH_3)PbI_3$ sensitized cells as a function of photoelectron density. Taken from ref. 16 with permission.

their efficiency. Graetzel and Park *et al.*[17] used the methyl ammonium lead iodide $CH_3NH_3PbI_3$ as light harvesters deposited onto a thick mesoscopic TiO_2 film including solid hole conductor (spiro-MeOTAD-2,2′,7,7′-tetrakis(*N*,*N*′-di-*p*-methoxyphenylamine)-9,9′-spirobifluorene) which was infiltrated the TiO_2 pores. This solid state sensitized perovskite-TiO_2 solar cell achieved PCE of 9.7% with J_{SC} of 17 mA cm^{-2} and V_{OC} of 0.888 V. The charge separation and hole injection were studied by femtosecond laser.

In other work on solid-state sensitized perovskite solar cells,[18] the influence of the TiO_2 thickness and the perovskite concentration on the photovoltaic performance was investigated. The authors found that when the TiO_2 film is decreased there is more pore filling which results in an increase in the V_{OC}; however, the optical density decreases. Fig. 3 presents UV-vis spectra and current voltage curves of the cells at various perovskite concentrations and TiO_2 film thicknesses. The change in the photocurrent observed is due to charge collection efficiency rather than light absorption. The conclusion was the same as for the liquid perovskite cell – when using thin TiO_2 film (completely filling pores) the photovoltaic performance was improved.

Ogomi *et al.*[19] passivated the porous titania with Y_2O_3 and with Al_2O_3. The passivation was done to remove surface traps of the porous titania to improve cells' efficiency. Measurements such as electron lifetime, thermally stimulated current, measurements of the microwave refractive carrier lifetime, and transient absorption spectroscopy were conducted. The authors show that surface passivation resulted in retardation of charge recombination between the electrons in the porous titania layers and the holes in the p-type organic conductors. Fig. 4 shows longer recombination time for the passivated porous titania compared to a nonpassivated surface.

Sero and Bisquert *et al.*[20] used impedance spectroscopy to separate the physical parameters of carrier transport and recombination of two kinds of perovskite solar cells using different morphologies and compositions. The first perovskite was $CH_3NH_3PbI_3$ with nanostructures of TiO_2, while the second cell was $CH_3NH_3PbI_{3-x}Cl_x$ perovskite deposited on top of a compact thin film of TiO_2. In their study, both cells showed the same V_{oc}, although the FF, J_{sc} and the efficiency were higher for the thin film TiO_2 cell.

Higher recombination rate was observed for the nanostructures of TiO_2 although the transport rate and conductivity were similar for both cells, indicating that the perovskite is more efficient pathway for transport (Fig. 5).

The authors determined the diffusion length for both cells using impedance spectroscopy. Both cells showed long

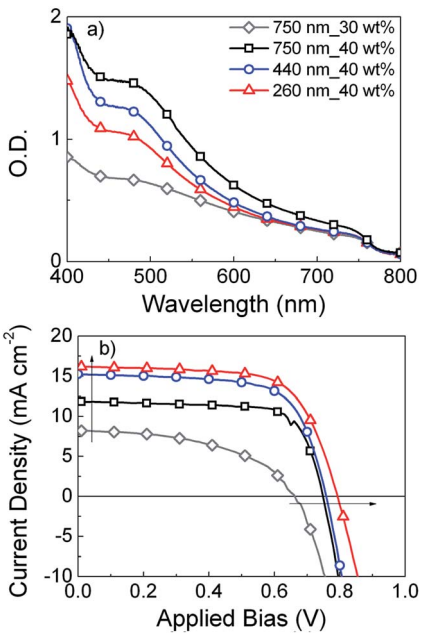

Fig. 3 UV-vis spectroscopy and current density *versus* voltage curves of the solar cells. (a) UV-vis spectra of the relevant solar cells (before electrode deposition) with a 750 nm TiO_2 scaffold (*m*-TiO_2) with 30 wt% perovskite precursor solution (gray diamonds), 750 nm TiO_2 with 40 wt% (black squares), 440 nm TiO_2 with 40 wt% (blue circles), 260 nm TiO_2 with 40 wt% (red triangles). These were taken in transmission mode in an integrating sphere to account for scattering. (b) Current density *versus* voltage curves of the same solar cells measured under 100 mW cm^{-2} simulated AM1.5 solar irradiation. Taken from ref. 18 with permission.

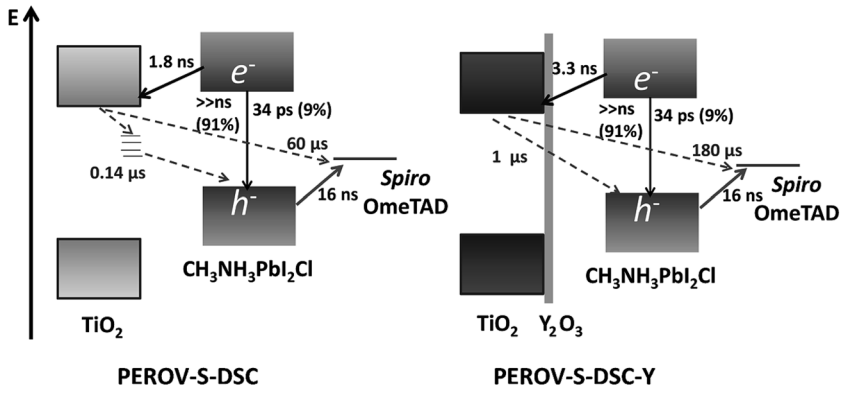

Fig. 4 Carrier dynamics of perovskite-sensitized solar cell before and after Y_2O_3 passivation. Taken with permission from ref. 19.

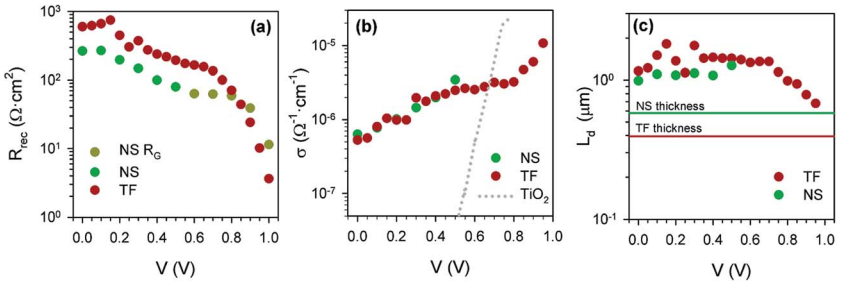

Fig. 5 Transport and recombination parameters *vs.* voltage: (a) recombination resistance, R_{rec}, (b) conductivity of active layer considering the geometric cell area, showing also the conductivity of nanostructured TiO_2 in a DSC with spiro-MeOTAD hole conductor, and (c) diffusion length for NS and TF cells. R_{tr} and R_{rec} cannot be unambiguously defined when Gerischer pattern is observed (NS sample for $V > 0.5$ V). Taken from ref. 20 with permission.

diffusion length of around 1 µm. In summary, the main difference between the morphologies, according to the interpretation of the impedance spectroscopy, is the higher recombination rate of the cells made with nanostructures of TiO_2 film.

In addition to optical and electrochemical measurements, the structure of the perovskite after its deposition on the mesoporous metal oxide was investigated. Lindblad and Rensmo *et al.*[21] measured the electronic structure and chemical composition of mesoporous TiO_2 in $CH_3NH_3PbI_3$ perovskite solar cells using hard X-ray photoelectron spectroscopy. The authors compared the one step deposition with the two step deposition and found similar stoichiometry and electronic structure. It was also shown that after perovskite deposition, the band gap states of TiO_2 are still present.

A further study of the structure of $CH_3NH_3PbI_3$ in mesoporous TiO_2 was done by Choi and Owen *et al.*[22] using atomic pair distribution function (PDF) analysis of high energy X-ray diffraction data. Only 30% of the perovskite consists of medium range ordered crystalline, tetragonal perovskite, while the remaining 70% forms a highly disordered phase within the mesoporous TiO_2 with short structural coherence of 1.4 nm. Moreover, the structure of the nano component was composed of small clusters of nanoparticles of two to eight octahedral lead iodide building blocks. The presence of disordered $CH_3NH_3PbI_3$ strongly affects the photoluminescence (PL) spectra, which also affects the photovoltaic performance.

Edri and Cahen *et al.*[23] used electron beam-induced current (EBIC) imaging to study the cell mechanism of $CH_3NH_3PbI_3$ and $CH_3NH_3PbI_{3-x}Cl_x$. They refer its structure to p–i–n devices. The authors extracted the diffusion length of electrons and holes from the EBIC contrast near the contacts (Fig. 6), and reveal that the diffusion length for holes is longer than the diffusion length for electrons with the former being at least 1 µm. This finding is in disagreement with diffusion length of *ca.* 100 nm as deduced earlier.[35,36] (Additional discussion about the diffusion length can be found in the next section.) As a result, the $CH_3NH_3PbI_3$ requires an electron conductor (mesoporous TiO_2) because of the short diffusion length of the electrons. In contrast, due to the long diffusion length of the holes, hole-transporting material is not essential.

4. Planar perovskite based solar cells

An interesting and notable observation regarding perovskite-based solar cells is the ability to use them in planar architecture, which means that sensitized architecture isn't necessarily the only option for the perovskite to function in a solar cell. The planar architecture eliminates infiltration problems of the perovskite and the hole transport material into the porous, which results in less recombination and better reproducibility. Planar architecture opens the way to implementation of other deposition techniques, as will described below. Fig. 7 show a

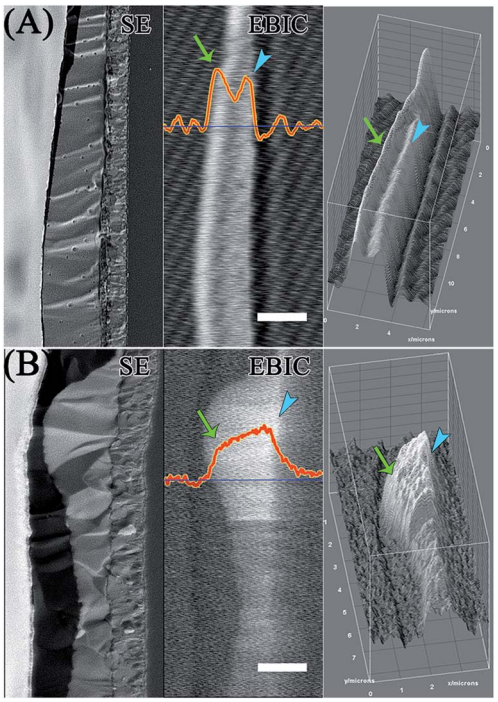

Fig. 6 SE and EBIC images of cross sections of $CH_3NH_3PbI_{3-x}Cl_x$ (A), scale bar is 2 μm, and $CH_3NH_3PbI_3$ (B), scale bar is 1 μm, planar solar cells. Line scans were taken at the lines' positions. The arrows show the peaks for the I–Cl and where the peaks are in the case of the pure iodide. The right panel is a 3D surface plot of the EBIC images. The ripples observed in the EBIC image of (A) outside the (semi-) conductive regions are due to background noise. Taken from ref. 23 with permission.

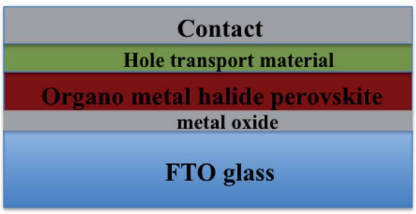

Fig. 7 Schematic illustration of the planar heterojunction perovskite solar cell.

schematic illustration of the layers involved in the planar architecture.

Lee and Snaith *et al.*[24] reported for the first time that the electron collector (TiO_2 metal oxide) isn't necessary for the operation of the perovskite solar cells. In their study, they used photo induced absorption (PIA) spectroscopy to examine the charge separation at the mesoporous TiO_2 and Al_2O_3 coated with perovskite with and without HTM. In the TiO_2 coated with perovskite, the PIA spectrum confirmed effective sensitization of the TiO_2 by the perovskite. Alternatively, Al_2O_3 coated with perovskite revealed no PIA signals, which confirmed the role of alumina as an insulator.

After adding the HTM, the oxidized species of the HTM (Spiro-OMETAD) created after photoexcitation of the perovskite were monitored. The research demonstrated that from the photoexcited perovskite to HTM the hole conductor is highly effective, and the hole transport material is necessary to enable long-lived charged species within the perovskite coated on Al_2O_3.

Moreover, small perturbation transient photocurrent decay measurements were performed to learn about the effectiveness of the perovskite as electronic charge transport. Charge collection in Al_2O_3 based devices was faster by a factor of >10 compared with TiO_2 based devices, indicating that the electron diffusion through the perovskite is faster in Al_2O_3 devices. The conclusion is that Al_2O_3 is simply acting as a scaffold for the device, which means that the perovskite solar cell demonstrated in this work is not a sensitized solar cell. The authors refer the Al_2O_3 cells as mesosuperstructured.

Low temperature planar perovskite solar cell was demonstrated using graphene flakes and presynthesized TiO_2 nanoparticles.[25] The reported efficiency was 15.6%, comparable to high temperature sintering process of TiO_2 based devices. The graphene + TiO_2 electrodes showed lower series resistance than the TiO_2 electrodes; moreover, the recombination resistance was higher in the case of the graphene + TiO_2 electrodes. The cross section of the device and its corresponding energy level diagram are presented in Fig. 8.

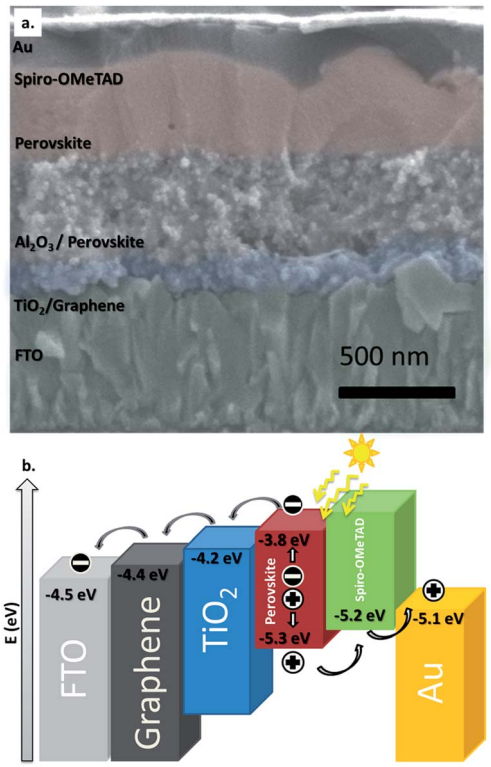

Fig. 8 (a) Cross-sectional SEM shows the device structure. (b) Energy level diagram of the described low temperature device. The authors indicate that these are the energy levels of the individual materials, and upon contact within the solar cell, there is likely to be a considerable relative shift.[26] Authors added that the graphene and TiO_2 were blended into a single composite layer and not layered as depicted in the energy level diagram. Taken from ref. 25 with permission.

Additional work on room temperature planar perovskite heterojunction solar cells was reported by using ZnO nanoparticles[27] as an alternative to both mesoporous TiO_2 and Al_2O_3 scaffolds. ZnO nanoparticles have a fabrication advantage due to the fact that they only need a spin coating step and do not require a heating and sintering step. Nanoparticles in the size range of 5 nm were made by hydrolysis of zinc acetate in methanol. Optimal film thickness was found to be around 25 nm and further increases in thickness did not improve PCE. The best PCE was found to be 15.7% with a 25 nm film thickness which was achieved by doing three spin coating layers. The cells were prepared similarly to most planar heterojunction perovskite cells, where the perovskite was deposited on the ZnO layer; then the HTM layer was deposited on top of the perovskite. PCE of 10.2% was found when this fabrication technique was employed on a flexible substrate made of ITO/PET. A recent work on low temperature (sub 150 °C) with meso-superstructured perovskite solar cells demonstrate slightly improved efficiency of 15.9%.[28]

The use of the planar architecture in flexible device was demonstrated[29] using $CH_3NH_3PbI_{3-x}Cl_x$, which was sandwiched between two organic contacts. The device structure employed (Fig. 9) was deemed "inverted" from regular device structure. The FTO was first coated with p-type material on top perovskite film, followed by n-type layer, finally aluminum was coated on top for the anode. Several p and n type contacts were studied. The best combination was PEDOT:PSS as the p-type layer and a bilayer of PCBM with a compact layer of TiO_x as the n-type layer. The titanium was employed only to create a stable electrical contact with the anode. The power conversion achieved for this "inverted" structure was 9.8%, with optimal perovskite film thickness of 300–400 nm. The efficiency of this design was slightly lower than that of the regular cells structure due to a slightly lower FF.

An interesting example for planar heterojunction perovskite solar cells is the ability to form semitransparent planar heterojunction solar cells with high efficiency.[31] Semi-transparent solar cells can be integrated, for instance, into windows and automotive applications. In order to make semi-transparent perovskite solar cells, it is essential to control the morphology of the perovskite thin film. One way to do that is to make perovskite "islands" which are small enough to appear continuous to the eye, but large enough to absorb the light to deliver high power conversion efficiency. The authors indicate that despite the observed voids in the films, high open circuit voltage and approximately 8% efficiency with 10% average of visible transmittance of the full device was observed.

As mentioned earlier one of the attractive properties of the perovskite is the ability to tune its optical properties by chemical modifications. One possible way to do it is to substitute the Pb with Sn, which results in an additional benefit, the reduction of the toxicity. Perovskite of the structure $CH_3NH_3Sn_xPb_{(1-x)}I_3$ was formed,[32] in which both the conduction and valence bands are shifted, and are shallower than those of titania by ~ -0.4 eV. Power conversion efficiency of 4.18% was achieved for the perovskite having the chemical formula of $CH_3NH_3Sn_{0.5}Pb_{0.5}I_3$.

In this configuration, Spiro-OMETAD could not be successfully employed as an HTM due to having a HOMO level that was deeper than that of the perovskite. This made hole injection into the HTM difficult; therefore, P3HT was employed as an HTM instead. The IPCE curve shifted to 1060 nm in the best performing Sn-halide perovskite, compared to $CH_3NH_3PbI_3$, which has an IPCE edge of 800 nm. Fig. 10 show the absorbance spectra of the several perovskite compositions.

Two recent reports showed complete substitution of the Pb by Sn which results with a lead free perovskite solar cell. In these reports the power conversion efficiency achieved was around 6%.[33,34]

The diffusion length of the electrons and holes was calculated[35,36] to be more than 1 μm for $CH_3NH_3PbI_{3-x}Cl_x$, justifying the high efficiency of the perovskite solar cell. As mentioned earlier different measurements techniques provide a variation

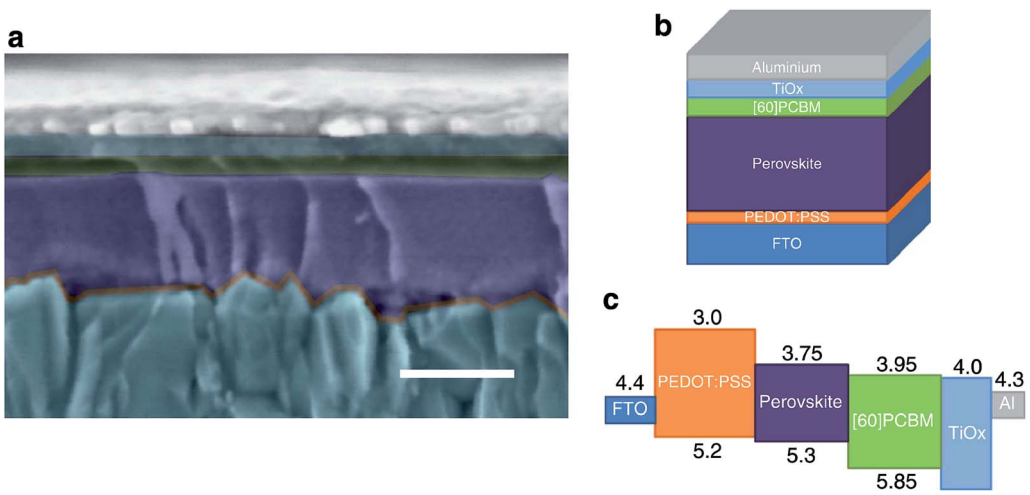

Fig. 9 (a) Cross section of the inverted planar perovskite solar cell. Scale bar represents 250 nm. The different layers have been tinted with the color scheme of the device schematic shown in (b). (c) Approximate energy band diagram of the fabricated inverted structure taken from ref. 30. The figure was taken from ref. 29 with permission.

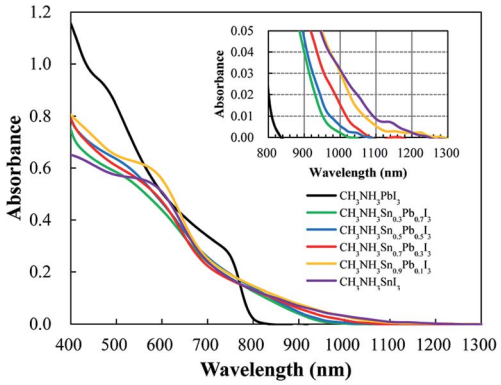

Fig. 10 Absorption spectra of $CH_3NH_3Sn_xPb_{(1-x)}I_3$ perovskite coated on porous TiO_2. Taken from ref. 32 with permission.

in the calculated diffusion length, moreover the deposition technique also influence the diffusion length as indicated by Yang *et al.*[43] and Snaith *et al.*[42] It is clear that long diffusion length of both carriers enables the use of the planar architecture.

The ability of perovskite to conduct both electrons and holes is an exceptional, distinctive property. This ability has been supported by the measurements of the long diffusion length of both carriers.[20,35,36] The ability to conduct both electrons and holes simplifies the device structure, enhancing the stability and eliminating the need to deal with infiltration issues of the HTM. The structure of the hole conductor free perovskite solar cell is presented in Fig. 11. Several research groups have already demonstrated enhanced PV performance of these hole conductor free perovskite solar cells, the highest PCE observed was 10.85%.[37–40] The current–voltage curve of the best PV performance is presented in Fig. 11B. Additionally, it appears that changing the halides in the perovskite (which influence its band gap) does not reduce its ability to conduct the electrons

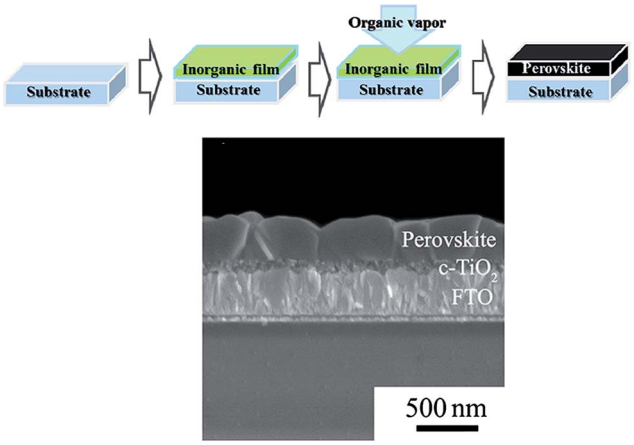

Fig. 13 Scheme of the vapor assisted solution process (VASP) technique and SEM cross section of the planar perovskite based solar cell. Taken from ref. 43 with permission.

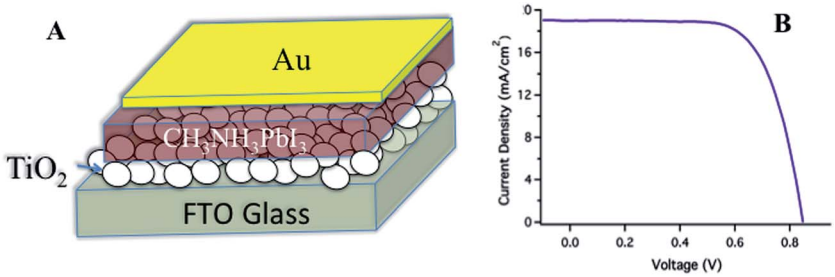

Fig. 11 (A) The structure of the perovskite solar cells without a hole conductor. (B) Current voltage of the 10.8% efficiency for hole conductor free perovskite solar cells. Taken from ref. 38 and 39 with permission.

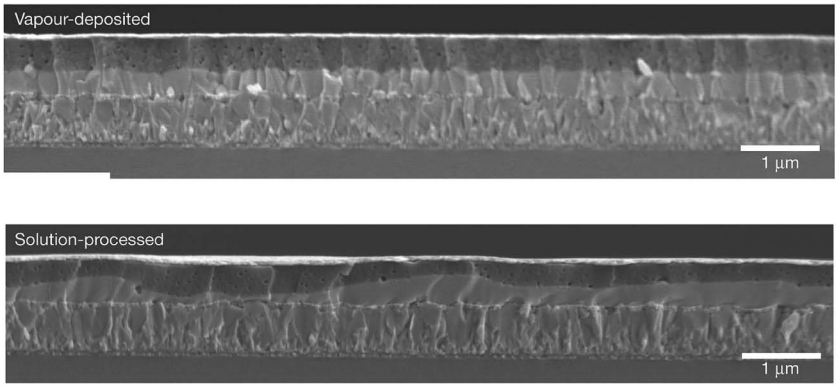

Fig. 12 Cross section of devices made by the two different deposition techniques. Taken from ref. 42 with permission.

Table 1 Comparison of the key parameters in the discussed architectures

	Sensitized architecture	Planar architecture
Operation mechanism	Still not yet completely understood	Still not yet completely understood
Electron-hole diffusion length	Calculated to be the same for both architectures	Calculated to be the same for both architectures
Solid hole transport material	Used for both	Used for both
Liquid electrolyte	Used in this architecture	Not used
Solution processed deposition techniques	Used in this architecture	Used in this architecture
Infiltration of perovskite and HTM	Infiltration difficulties	No infiltration problems
Recombination	Higher recombination than the planar structure. The amount of pore filling determines the rate of recombination	Less recombination than the sensitized architecture
Metal oxide thickness	Thicker metal oxide films	Thin metal oxide films
Flexible devices	Was not demonstrated yet	Used in this architecture
Vapor deposition	Not used	Used in this architecture
Vapor-assisted solution processed technique-VASP	Not used	Used in this architecture
Semitransparent devices	Was not demonstrated yet	Used in this architecture

and holes as proved by its implementation in the hole conductor free devices.[41]

Vapor deposition technique was investigated for planar heterojunction perovskite solar cells achieving high efficiency.[42] A comparison between the vapor deposition technique and the solution-processed technique was reported. For the vapor deposition technique, the film was stacked and uniform with a thickness of ~330 nm. While for the solution-processed film, the thickness ranged between 50–410 nm and non-uniform. This is the explanation for the difference in performance; in the case of solution processed film, the voids in the perovskite layer lead to direct contact between the polymer and the TiO_2 causing shunt path, that is, in part, responsible for lowering cell performance (Fig. 12).

Except the vapor deposition technique mentioned, Chen and Yang *et al.*[43] demonstrate the use of the vapor assisted solution process (VASP) to fabricate the planar devices based on perovskite. This deposition technique requires the solution deposition of PbI_2 with CH_3NH_3I vapor (see Fig. 13). The important point regarding the VASP technique is avoiding co-deposition of organic and inorganic species. Using this technique, the perovskite films are well defined with full surface coverage and low surface roughness that make them suitable for PV applications. Planar perovskite solar cells based on the VASP technique achieved PCE of 12.1%.

5. Summary and outlook

The fast growth of perovskite based solar cells in the recent years exhibits its potential to compete with the current technologies as a possible solution for solar energy.

Organo-metal halide perovskite has several advantages, making it an excellent candidate for use in photovoltaic solar cells. Its high absorption coefficient, optical band gap tuning, direct band gap, high stability, high carrier mobility, and the ability to use it in different device structures are important, even ideal, properties for a successful light harvester in a solar cell.

Further, perovskite does not require expensive and complicated techniques, but results from simple preparation, such as solution processed, spin coating or printing. In addition, the perovskite can be made under low temperature fabrication. These advantages position perovskite as a promising material for photovoltaic devices, superior to the current technologies—including organic PV, DSSC and even silicon solar cells.

Beyond these important properties, organo-metal halide perovskite isn't restricted to specific solar cell architecture. It can deliver high power conversion efficiencies in two main device structures, as described in this review—sensitized solar cell structure (originally came from the DSSC technology), and planar solar cell structure, indicated as thin film cells, or even in some cases, as extremely thin absorber cells. The following table summarizes the main points related to the architectures (Table 1).

It can be said that organo-metal halide perovskite is a game changer in the solar energy technology. In just three years its efficiency increased more than 16%, 20% efficiency is just around the corner and 22–23% efficiencies are attainable. Looking to the future, there are several ways to improve the perovskite-based solar cells. Perovskite deposition is a key issue to improve its coverage in order to achieve high efficiency cells. Tuning the band alignment between the different layers in the device could reduce energy losses and recombination. Increasing the charge density in the metal oxide film would improve charge separation and reduce the recombination rate. Finally, all device improvements should entail low cost techniques in keeping with the trend of the third generation cells. The ability to use perovskite in sensitized or planar architectures, in addition to its ambipolar properties, are definitely competitive advantages for achieving high power conversion efficiencies.

Acknowledgements

L.E. would like to thank the Israel Alternative Energy Foundation (I-SAEF), the Office of the Chief Scientist of the Ministry of

Industry, Trade and Labor Kamin, and the Tashtiot project by the Chief Scientist of the Ministry. L.E. would like to thank his research group and collaborators for contributing to the development of the perovskite based solar cells.

References

1 A. Kojima, K. Teshima, Y. Shirai and T. Miyasaka, Organometal Halide Perovskites as Visible-Light Sensitizers for Photovoltaic Cells, *J. Am. Chem. Soc.*, 2009, **131**, 6050–6051.

2 http://www.nrel.gov/ncpv/images/efficiency_chart.jpg.

3 J. Burschka, N. Pellet, S.-J. Moon, R. Humphry-Baker, P. Gao, M. K. Nazeeruddin1 and M. Graetzel, *Nature*, 2013, **499**, 316.

4 J. T.-W. Wang, J. M. Ball, E. M. Barea, A. Abate, J. A. Alexander-Webber, J. Huang, M. Saliba, I. Mora-Sero, J. Bisquert, H. J. Snaith and R. J. Nicholas, *Nano Lett.*, 2014, **14**, 724.

5 N. J. Jeon, H. G. Lee, Y. C. Kim, J. Seo, J. H. Noh, J. Lee and S. I. Seok, *o*-Methoxy Substituents in Spiro-OMeTAD for Efficient Inorganic–Organic Hybrid Perovskite Solar Cells, *J. Am. Chem. Soc.*, 2014, **136**(22), 7837–7840.

6 B. Cai, Y. Xing, Z. Yang, W.-H. Zhang and J. Qiu, High performance hybrid solar cells sensitized by organolead halide perovskites, *Energy Environ. Sci.*, 2013, **6**, 1480.

7 E. Edri, S. Kirmayer, D. Cahen and G. Hodes, High Open-Circuit Voltage Solar Cells Based on Organic–Inorganic Lead Bromide Perovskite, *J. Phys. Chem. Lett.*, 2013, **4**, 897–902.

8 A. S. Bhalla, R. Guo and R. Roy, The perovskite structure – a review of its role in ceramic science and technology, *Mater. Res. Innovations*, 2000, **4**, 3–26, and references therein.

9 D. B. Mitzi, *Synthesis, Structure, and Properties of Organic–Inorganic Perovskites and Related Materials, in Progress in Inorganic Chemistry*, John Wiley & Sons, Inc., New York, 1999, vol. 48, p. 1.

10 G. E. Eperon, S. D. Stranks, C. Menelaou, M. B. Johnston, L. M. Herz and H. J. Snaith, Formamidinium lead trihalide: a broadly tunable perovskite for efficient planar heterojunction solar cells, *Energy Environ. Sci.*, 2014, **7**, 982–988.

11 J. H. Noh, S. H. Im, J. H. Heo, T. N. Mandal and S. I. Seok, Chemical management for colorful, efficient, and stable inorganic–organic hybrid nanostructured solar cells, *Nano Lett.*, 2013, **13**, 1764–1769.

12 A. Kojima, M. Ikegami, K. Teshima and T. Miyasaka, Highly Luminescent Lead Bromide Perovskite Nanoparticles Synthesized with Porous Alumina Media, *Chem. Lett.*, 2012, **41**, 397.

13 C. R. Kagan, D. B. Mitzi and C. D. Dimitrakopoulos, Organic–Inorganic Hybrid Materials as Semiconducting Channels in Thin-Film Field-Effect Transistors, *Science*, 1999, **286**, 945.

14 D. B. Mitzi, C. A. Field, Z. Schlesinger and R. B. Laibowitz, Transport Optical and Magnetic properties of the conducting Halide Perovskite $CH_3NH_3SnI_3$., *J. Solid State Chem.*, 1995, **114**, 159.

15 J. H. Im, C. R. Lee, J. W. Lee, S. W. Park and N. G. Park, 6.5% efficient perovskite quantum-dot-sensitized solar cell, *Nanoscale*, 2011, **3**(10), 4088–4093.

16 Y. Zhao and K. Zhu, Charge Transport and Recombination in Perovskite $(CH_3NH_3)PbI_3$ Sensitized TiO_2 Solar Cells, *J. Phys. Chem. Lett.*, 2013, **4**, 2880–2884.

17 H.-S. Kim, C.-R. Lee, J.-H. Im, Ki-B. Lee, T. Moehl, A. Marchioro, S.-J. Moon, R. Humphry-Baker, J.-H. Yum, J. E. Moser, M. Graetzel and N.-G. Park, Lead Iodide Perovskite Sensitized All-Solid-State Submicron Thin Film Mesoscopic Solar Cell with Efficiency Exceeding 9%, *Sci. Rep.*, 2013, 591, DOI: 10.1038/srep00591.

18 T. Leijtens, B. Lauber, G. E. Eperon, S. D. Stranks and H. J. Snaith, The Importance of Perovskite Pore Filling in Organometal Mixed Halide Sensitized TiO_2 Based Solar Cells, *J. Phys. Chem. Lett.*, 2014, **5**, 1096–1102.

19 Y. Ogomi, K. Kukihara, S. Qing, T. Toyoda, K. Yoshino, S. Pandey, H. Momose and S. Hayase, Control of Charge Dynamics through a Charge-Separation Interface for All-Solid Perovskite-Sensitized Solar Cells, *ChemPhysChem*, 2014, **15**, 1062–1069.

20 V. Gonzalez-Pedro, E. J. Juarez-Perez, W.-S. Arsyad, E. M. Barea, F. Fabregat-Santiago, I. Mora-Sero and J. Bisquert, General Working Principles of $CH_3NH_3PbX_3$ Perovskite Solar Cells, *Nano Lett.*, 2014, **14**, 888–893.

21 R. Lindblad, D. Bi, B.-w. Park, J. Oscarsson, M. Gorgoi, H. Siegbahn, M. Odelius, E. M. J. Johansson and H. Rensmo, Electronic Structure of $TiO_2/CH_3NH_3PbI_3$ Perovskite Solar Cell Interfaces, *J. Phys. Chem. Lett.*, 2014, **5**, 648–653.

22 J. J. Choi, X. Yang, Z. M. Norman, S. J. L. Billinge and J. S. Owen, Structure of Methylammonium Lead Iodide Within Mesoporous Titanium Dioxide: Active Material in High-Performance Perovskite Solar Cells, *Nano Lett.*, 2014, **14**, 127–133.

23 E. Edri, S. Kirmayer, A. Henning, S. Mukhopadhyay, K. Gartsman, Y. Rosenwaks, G. Hodes and D. Cahen, Why Lead Methylammonium Tri-Iodide Perovskite-Based Solar Cells Require a Mesoporous Electron Transporting Scaffold (but Not Necessarily a Hole Conductor), *Nano Lett.*, 2014, **14**, 1000–1004.

24 M. M. Lee, J. Teuscher, T. Miyasaka, T. N. Murakami and H. J. Snaith, Efficient Hybrid Solar Cells Based on Meso-Superstructured Organometal Halide Perovskites, *Science*, 2012, **338**, 643–647.

25 J. T.-W. Wang, J. M. Ball, E. M. Barea, A. Abate, J. A. Alexander-Webber, J. Huang, M. Saliba, I. À. Mora-Sero, J. Bisquert, H. J. Snaith and R. J. Nicholas, Low-Temperature Processed Electron Collection Layers of Graphene/TiO_2 Nanocomposites in Thin Film Perovskite Solar Cells, *Nano Lett.*, 2014, **14**, 724–730.

26 X. Wang, L. Zhi and K. Muellen, *Nano Lett.*, 2008, **8**(1), 323–327.

27 D. Liu and T. L. Kelly, Perovskite solar cells with a planar heterojunction structure prepared using room-temperature solution processing techniques, *Nat. Photonics*, 2014, **8**, 133–138.

28 K. Wojciechowski, M. Saliba, T. Leijtens, A. Abate and H. J. Snaith, Sub-150C processed meso-superstructured perovskite solar cells with enhanced efficiency, *Energy Environ. Sci.*, 2014, **7**, 1142.

29 P. Docampo, J. M. Ball, M. Darwich, G. E. Eperon and H. J. Snaith, Efficient organometal trihalide perovskite planar-heterojunction solar cells on flexible polymer substrates, *Nat. Commun.*, 2013, **4**, 2761.

30 A. Abrusci, *et al.*, High performance perovskite-polymer hybrid solar cells *via* electronic coupling with fullerene monolayers, *Nano Lett.*, 2013, **13**, 3124–3128.

31 G. E. Eperon, V. M. Burlakov, A. Goriely and H. J. Snaith, Neutral Color Semitransparent Microstructured Perovskite Solar Cells, *ACS Nano*, 2014, **8**, 591–598.

32 Y. Ogomi, A. Morita, S. Tsukamoto, T. Saitho, N. Fujikawa, Q. Shen, T. Toyoda, K. Yoshino, S. S. Pandey, T. Ma and S. Hayase, $CH_3NH_3Sn_xPb_{(1-x)}I_3$ Perovskite Solar Cells Covering up to 1060 nm, *J. Phys. Chem. Lett.*, 2014, **5**, 1004–1011.

33 N. K. Noel, S. D. Stranks, A. Abate, C. Wehrenfennig, S. Guarnera, A. Haghighirad, A. Sadhanala, G. E. Eperon, S. K. Pathak, M. B. Johnston, A. Petrozza, L. Herz and H. Snaith, Lead-Free Organic-Inorganic Tin Halide Perovskites for Photovoltaic Applications, *Energy Environ. Sci.*, 2014, DOI: 10.1039/c4ee01076k.

34 F. Hao, C. C. Stoumpos, D. Hanh Cao, R. P. H. Chang and M. G. Kanatzidis, Lead-free solid-state organic–inorganic halide perovskite solar cells, *Nat. Photonics*, 2014, **8**, 489.

35 G. Xing, N. Mathews, S. Sun, S. Sien Lim, Y. Ming Lam, M. Grätzel, S. Mhaisalkar and T. Chien Sum, Long-Range Balanced Electron- and Hole-Transport Lengths in Organic-Inorganic $CH_3NH_3PbI_3$, *Science*, 2013, **342**, 344.

36 S. D. Stranks, G. E. Eperon, G. Grancini, C. Menelaou, M. J. P. Alcocer, T. Leijtens, L. M. Herz, A. Petrozza and H. J. Snaith, Electron-Hole Diffusion Lengths Exceeding 1 Micrometer in an Organometal Trihalide Perovskite Absorber, *Science*, 2013, **342**, 34–344.

37 J. Shi, J. Dong, S. Lv, Y. Xu, L. Zhu, J. Xiao, X. Xu, H. Wu, D. Li, Y. Luo and Q. Meng, Hole-conductor-free perovskite organic lead iodide heterojunction thin-film solar cells: High efficiency and junction property, *Appl. Phys. Lett.*, 2014, **104**, 063901.

38 S. Aharon, S. Gamliel, B. E. Cohen and L. Etgar, Depletion region effect of highly efficient hole conductor free $CH_3NH_3PbI_3$ perovskite solar cells, *Phys. Chem. Chem. Phys.*, 2014, **16**, 10512–10518.

39 W. Abu Labana and L. Etgar, Depleted hole conductor-free lead halide iodide heterojunction solar cells, *Energy Environ. Sci.*, 2013, **6**, 3249–3253.

40 L. Etgar, P. Gao, Z. Xue, Q. Peng, A. K. Chandiran, B. Liu, Md. K. Nazeeruddin and M. Grätzel, Mesoscopic $CH_3NH_3PbI_3/TiO_2$ Heterojunction Solar Cells, *J. Am. Chem. Soc.*, 2012, **134**(42), 17396–17399.

41 S. Aharon, B.-E. Cohen and L. Etgar, Hybrid Lead Halide Iodide and Lead Halide Bromide in Efficient Hole Conductor Free Perovskite Solar Cell., *J. Phys. Chem. C*, 2014, DOI: 10.1021/jp5023407.

42 M. Liu, M. B. Johnston and H. J. Snaith, Efficient planar heterojunction perovskite solar cells by vapour deposition, *Nature*, 2013, **501**, 395–399.

43 Q. Chen, H. Zhou, Z. Hong, S. Luo, H.-S. Duan, H.-H. Wang, Y. Liu, G. Li and Y. Yang, Planar Heterojunction Perovskite Solar Cells *via* Vapor-Assisted Solution Process, *J. Am. Chem. Soc.*, 2014, **136**, 622–625.